

Some statistical properties of small scale turbulence in an atmospheric boundary layer

By R. W. STEWART, J. R. WILSON AND R. W. BURLING

Institute of Oceanography University of British Columbia
Vancouver, Canada

(Received 3 September 1969)

Derivatives of velocity signals obtained in a turbulent boundary layer are examined for correspondence to the lognormal distribution. It is found that there is rough agreement but that unlikely events at high values are much less common in the observed fields than would be inferred from the lognormal distribution. The actual distributions correspond more to those obtained from a random walk with a limited number of steps, so the difference between these distributions and the lognormal may be related to the fact that the Reynolds number is finite.

The third-order structure function is examined, and found to be roughly consistent with the existence of an inertial subrange of a Kolmogoroff equilibrium régime over a range of scale which is *a priori* reasonable but which is far less extensive than the $-\frac{5}{3}$ region of the spectrum.

Introduction

The local dissipation rate per unit mass in a turbulent field is defined, in the usual notation, as

$$\epsilon = \frac{1}{2}\nu \overline{\left(\frac{\partial u_i}{\partial x_j} + \frac{\partial u_j}{\partial x_i}\right)^2}.$$

Because of the number of terms in the expression this quantity is very difficult to measure experimentally. For this reason information about it is usually inferred by observing some other quantity which there is reason to believe behaves in a similar manner. The quantity usually used is some sort of short term average of a velocity derivative such as

$$\frac{\partial u_1}{\partial x_1} \quad \text{or} \quad \frac{\partial u_3}{\partial x_1}.$$

It has been noted for some time that these quantities and others like them, when averaged over a suitably small volume, are random variables with distributions which are decidedly non-Gaussian. In particular, they are characterized by a high coefficient of excess.

Shortly after the development of the similarity theories of Kolmogorov (1941) and Oboukhov (1941*a*) it was pointed out by Landau that the variation of ϵ caused some difficulty. Subsequently Kolmogorov (1962) and Oboukhov (1962) modified their theories to take this factor into account. The modifications involved

the assumption that the logarithm of ϵ was a normally distributed quantity, although no theoretical evidence for this assumed behaviour was presented at the time. Still later Novikov & Stewart (1964) considered a model of the turbulence based purely on the experimentally observed nature of the dissipation rate. By subdividing space into a series of smaller and smaller volumes and assuming that for each stage of subdivision random volumes had either zero dissipation or some constant dissipation they were able to predict that the spectrum of the fluctuations of ϵ would exhibit a power law behaviour with the parameter between 0 and -1 . Some measurements of quantities which should have behaved like ϵ were made by Pond (1965) and seemed to bear this out.

The latest contribution to the theory of the spatial and time variation of ϵ has been offered by Gurvich & Yaglom (1967). Their paper presents a theoretical treatment leading to the predictions that certain quantities, including the dissipation rate, should have the logarithmic-normal probability distribution and that the spectrum of the square of these quantities should have a power law behaviour.

The present paper is an account of some of the results of an experiment undertaken to test the validity of the lognormal theory. Some other results concerning the structure functions and the higher moments of the velocity derivatives have been included.

Data

Observational data for velocity fluctuations were collected in the atmospheric boundary layer over the ocean, using a Disa constant temperature hot wire anemometer. Wire diameter was 5μ and length 1 mm, permitting good measurements down to scale sizes of less than 0.5 cm. The probe was mounted at heights of 1.5 to 2 metres above the water and the measurements were made in various mean wind speeds ranging from 4 to 8 m/sec. The velocity signal was differentiated by analogue means and recorded as an FM signal at $7\frac{1}{2}$ in./sec on an Ampex FR-1300 tape recorder.

Care was taken to maintain the wave form of the signal in order to obtain the true distribution. The filters used to remove high frequency noise prior to differentiation were chosen to have a phase shift linear with frequency over the band of interest. The total phase shift of the circuit was measured to be within one or two degrees of linear in the band 0 to 2000 Hz.

Analysis of the data was accomplished through the use of a 10 bit analogue to digital converter. The signal was filtered with the linear phase shift filter to minimize aliasing and digitized at a rate to provide spectrum information out to the highest frequencies for which the recorded signal was discernible from the noise. Considerable care was taken in recording, reproducing and digitizing to ensure that no clipping occurred. The extreme peak-to-peak excursions of the signal occupied less than two-thirds of the dynamic range of all instruments used.

Figure 1 shows a typical spectrum of the differentiated velocity. The filter used in both recording and digitizing had a 3 db point at 2000 Hz. The 3 db point

of the FM system of the tape recorder was above 2500 Hz. Therefore, only the last 3 or 4 points of the spectrum shown in figure 1 are significantly affected by the filters, indicating that the signal is relatively noise free and that nearly all the dissipation range has been included.

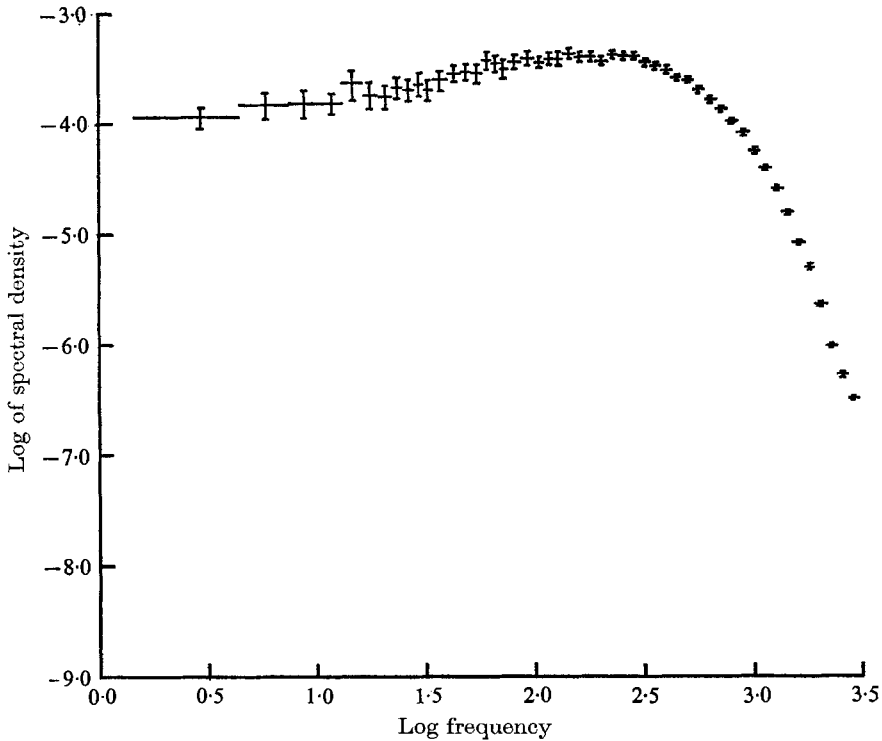


FIGURE 1. Spectrum of the differentiated downstream velocity fluctuations. Mean wind was 8.3 m/sec.

Results

In the following presentation of the results the probability density functions have been constructed for the logarithm of the absolute value of the differentiated downstream velocity fluctuations. The predictions of Gurvich & Yaglom are in terms of the logarithm of the square of this quantity. It can easily be shown, however, that if a quantity has a logarithmic-normal distribution its positive square root also has a lognormal distribution. Use of the absolute value allowed a more direct comparison of the observed and theoretical even moments of the signal.

Figure 2 shows a typical observed probability density function of this logarithm. The bar graph represents the observed data. The smooth curve is the best fit of a curve of the normal type to points located in the centre of each bar. In forming the distributions the mean of the differentiated signal was chosen as its zero; its positive and negative sides were then treated separately for simplicity in the analysis. Figure 2 shows the negative side of the signal. The positive side

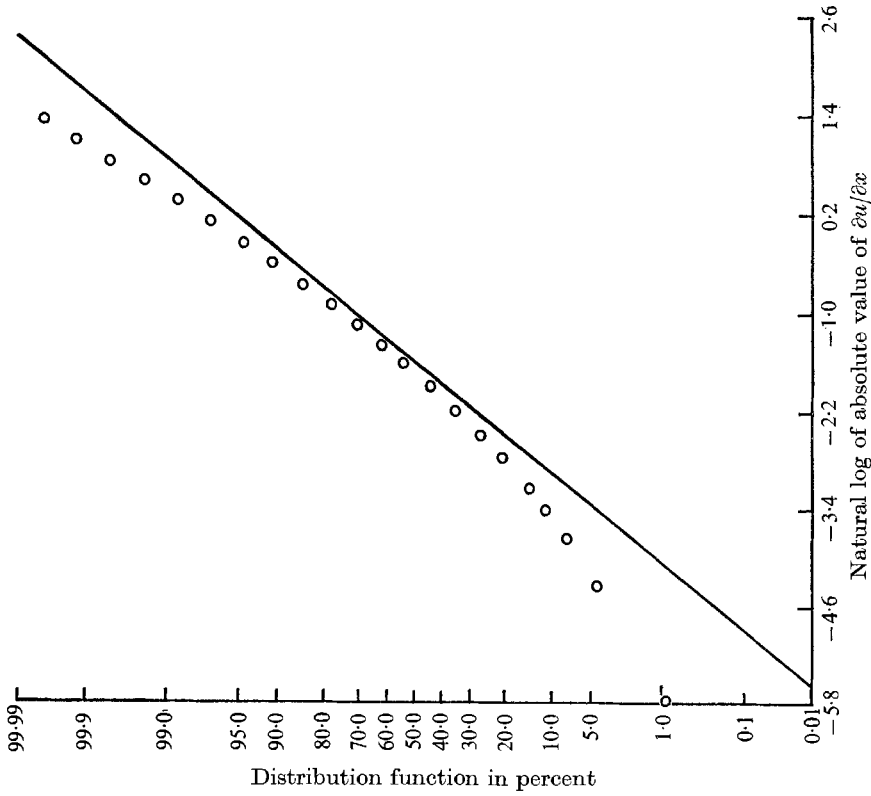


FIGURE 3. Arithmetic probability plot for the velocity data. The straight line corresponds to the least squares fit of figure 2.

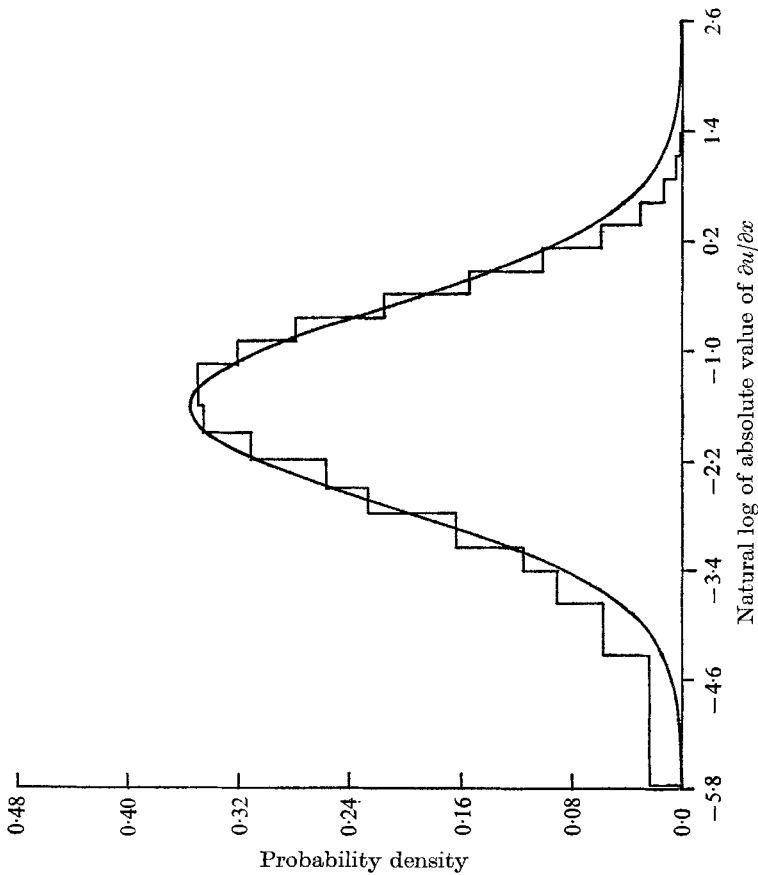


FIGURE 2. Probability density function for the velocity data. The bar graph is the observed distribution and the smooth curve is the best (least squares) normal curve.

is qualitatively identical. From the results of the separate cases it could later be seen that increasing the sophistication of the computation to produce a distribution of the total signal would not affect significantly the nature of the departure of the results from the theoretical prediction.

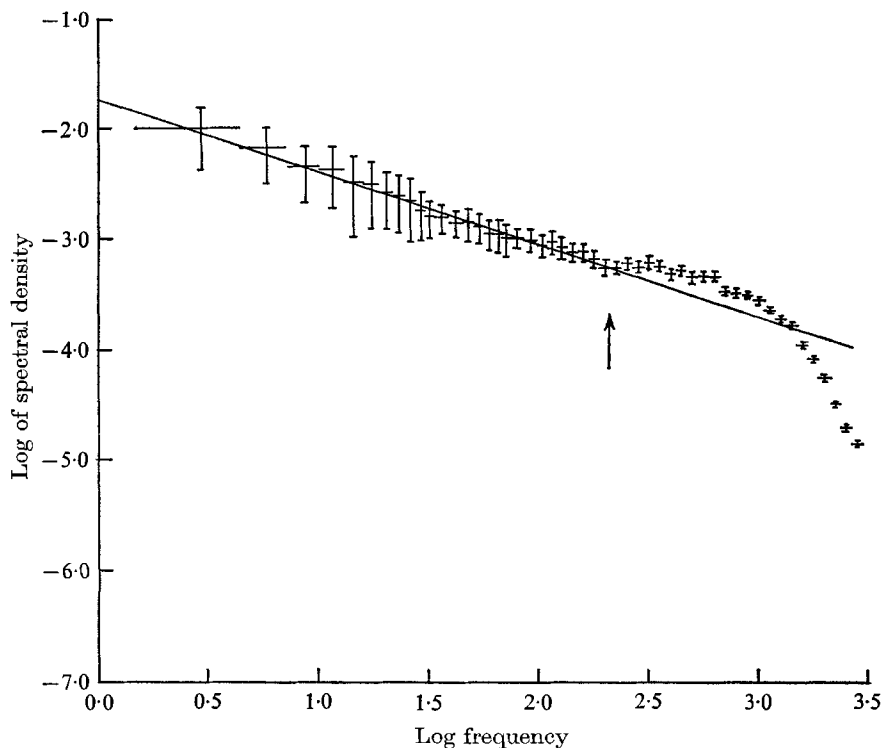


FIGURE 4. Spectrum of the square of the differentiated downstream velocity fluctuations. The vertical arrow represents the peak of the dissipation spectrum.

Section	Skewness	Coefficient of excess†	Time (sec)
1	-0.69	13.1	240
2	-0.71	12.3	240
3	-0.56	9.3	120
4	-0.76	17.9	90
5	-0.71	16.6	120
6	-0.56	10.6	515

TABLE 1. Differentiated velocity

† In previous publications from this Institute we have used the word 'kurtosis' for 'coefficient of excess'. Because 'kurtosis' has at least three definitions in reputable literature we suggest that the word be avoided and that henceforth 'coefficient of excess' be used for:

$$\overline{e^4}/(\overline{e^2})^2 - 3$$

and that the term 'flatness factor', which has a long and respectable history in the turbulence literature be used for $\overline{e^4}/(\overline{e^2})^2$.

Figure 3 is the corresponding arithmetic probability plot for the same data. The straight line on this plot corresponds to the normal distribution computed in the least squares fit of figure 2.

Table 1 shows the values obtained for skewness and kurtosis for each section of differentiated velocity data analyzed. The length in seconds of each section is also given. Figure 2 corresponds to section 6 of the velocity data.

These differentiated velocity data can also be used to determine the spectral behaviour of the quantities related to ϵ .

Figure 4 is the spectrum of the square of the downstream differentiated velocity fluctuations. The straight line has a slope of -0.65 .

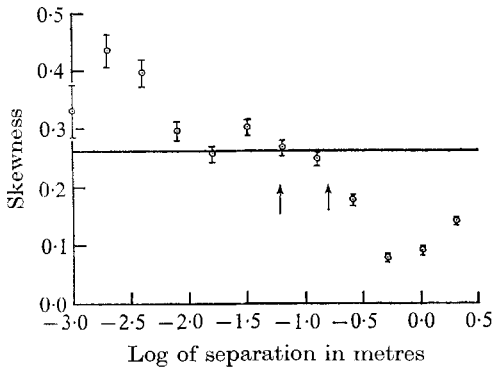


FIGURE 5

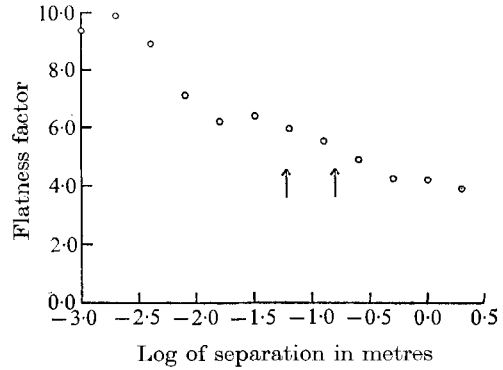


FIGURE 6

FIGURE 5. Skewness for the downstream velocity structure function. The left vertical arrow corresponds to one 'wavelength' at the frequency of the peak of the spectrum. The other vertical arrow represents one-tenth of the height of the probe above the water.

FIGURE 6. Flatness factor of the downstream velocity structure function. The vertical arrows correspond to those of figure 5.

Structure functions

The undifferentiated velocity signals were also recorded during the observational period. A calculation of structure functions from these signals permits the values of skewness and coefficient of excess of the derivative to be put into a broader context. They are also of some interest in themselves. Taylor's hypothesis was assumed in computing the two-point downstream velocity differences.

The normalized third-order structure function (skewness) is given by

$$\frac{\overline{(\mu_1 - \mu'_1)^3}}{[\overline{(\mu_1 - \mu'_1)^2}]^{3/2}}$$

The normalized fourth-order structure function (flatness factor) is given by

$$\frac{\overline{(\mu_1 - \mu'_1)^4}}{[\overline{(\mu_1 - \mu'_1)^2}]^2}$$

Figures 5 and 6 show typical results (for section 1 of the data) for the normalized third- and fourth-order structure functions as a function of logarithm of separation.

Discussion

As can be seen from figure 2 the logarithmic-normal distribution describes the derivative of velocity reasonably well. There, is, however, a significant deviation from the form particularly for very small and very large values. The observed logarithms represented by the bar graph in figure 2 have a skewness of -0.49 and a coefficient of excess of 0.02 .

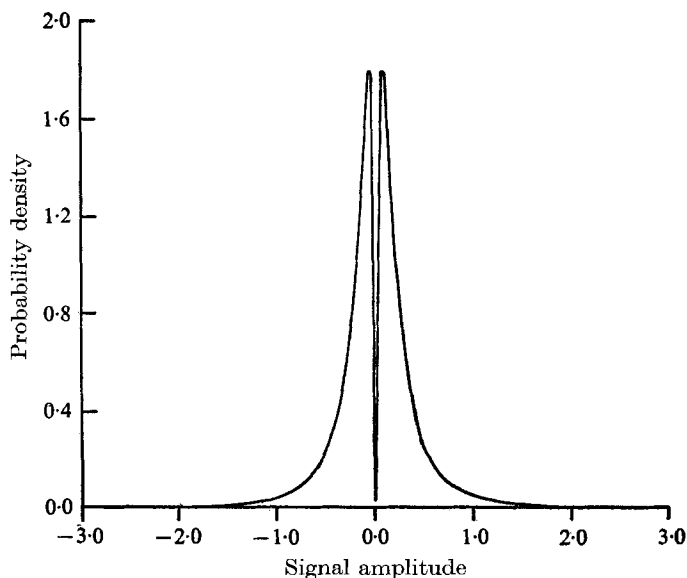


FIGURE 7. Two sided probability density function for a logarithmic-normally distributed variable.

The excess of small values is not unexpected due to the nature of this distribution. Figure 7 is an example of a theoretical logarithmic-normal distribution with parameters very nearly equal to typical observed values. The distribution shows small values of the probability in the neighbourhood of zero and the largest values of probability for very nearby values. The electronic noise associated with the tape recorder alone is of the order of the separation between the peak of the distribution and zero. Therefore, we would expect the noise adding independently to the signal to tend to fill in the gap about zero and produce an excess of small values. Figure 8 shows the theoretical result of adding independently a logarithmic-normally distributed quantity very similar to those experimentally obtained and a normally distributed quantity similar to the circuit noise. It can be seen that the effect of noise 'penetrates' to values of $\ln x$ equal to about -2.5 , and can in no way account for all of the difference from lognormal seen in figures 2 and 3.

This may account for the behaviour at small values, but it in no way accounts for the observed deficiency of large values. Another 'explanation' may be suggested for this region:

The argument advanced by Gurvich & Yaglom for the existence of the logarithmic-normal distribution is based on a subdivision of space into smaller and smaller volumes, one located inside the other. The ratio of the dissipation in a volume to that in the immediately larger volume in which it is located is then examined as a statistical variable.

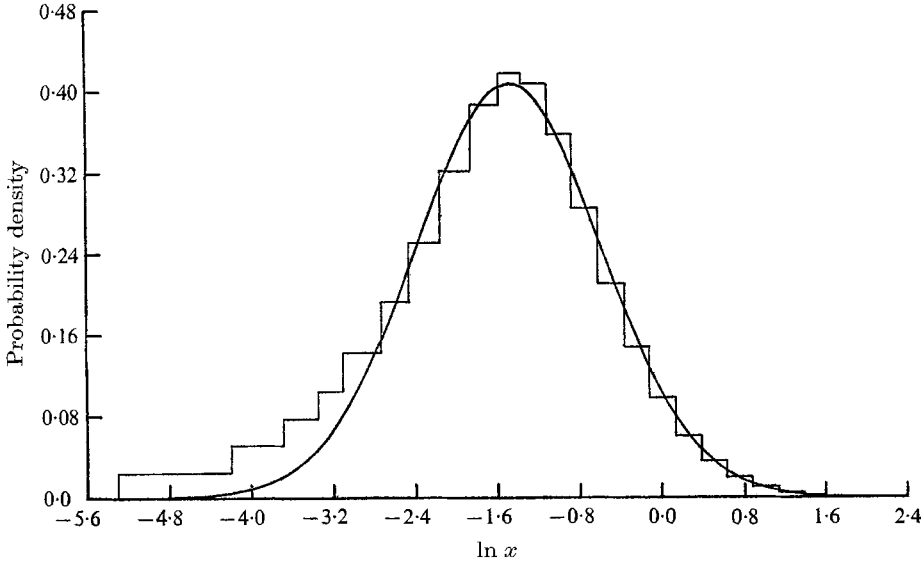


FIGURE 8. Effect of a small Gaussian noise adding independently to a lognormally distributed variable. The smooth curve is the best least-squares normal curve for comparison.

If α_j is the ratio of the average of ϵ in a volume of the j subdivision to the average of ϵ in the $j-1$ subdivision and if there are n stages of subdivision then

$$\bar{\epsilon}_n = \epsilon_0 \alpha_1 \alpha_2 \dots \alpha_n$$

and

$$\log \bar{\epsilon}_n = \log \epsilon_0 + \sum_{i=1}^n \log \alpha_i.$$

If the Reynolds number is high enough so that n is a large enough number and if the $\log \alpha_j$ are independent and are assumed to have finite means and variances then the central limit theorem is applicable and $\log \bar{\epsilon}_n$ should tend towards the normal distribution. If the Reynolds number and therefore n is not high enough, we might expect a deficiency of large values to occur because of the limit on how large $\log \bar{\epsilon}_n$ can become. For small values of n the distribution will tend to approach that of α_j . If this distribution is also lognormal then of course the overall distribution will be lognormal regardless of n . However, there is no reason to expect this to be the case, and the internal evidence is against it.

To test this idea a series of random numbers was generated and multiplied together on a computer. For the reasons given above the logarithm of this

product could be expected to have a distribution which would approach normal as the number of random numbers used increased. Some insight into the effect of a small Reynolds number could then be obtained by limiting the number of random numbers in the product. The probability density function from which the numbers were drawn was defined by:

$$\begin{aligned}
 P(x) &= 0 & (x < x_a); \\
 P(x) &= 1/(x_b - x_a) & (x_a \leq x \leq x_b); \\
 P(x) &= 0 & (x > x_b).
 \end{aligned}$$

x_a and x_b were chosen so that the first two moments of the resulting distribution of the product of the numbers corresponded closely to the experimental distributions.

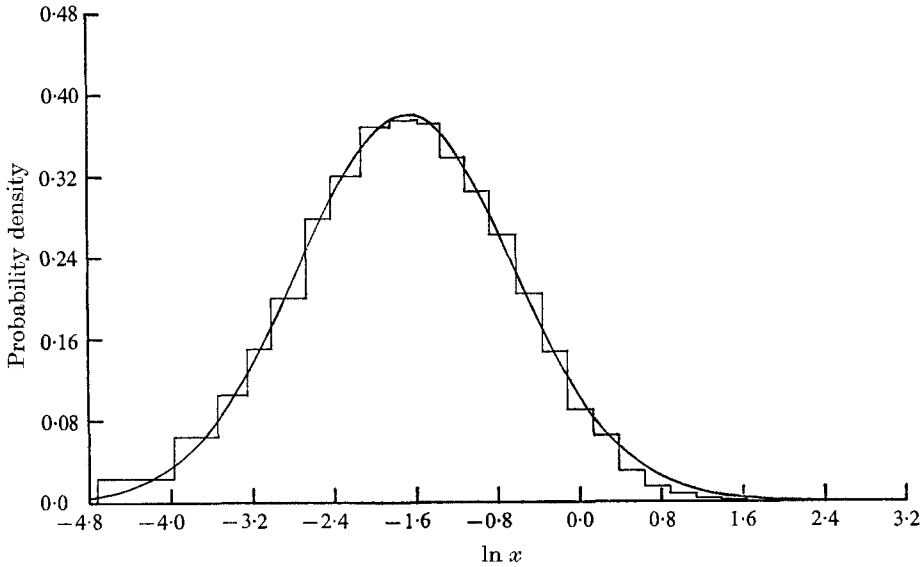


FIGURE 9. Distribution of the product of ten random numbers. The smooth curve is the best least squares normal curve for comparison.

Figure 9 shows one such distribution for a product of 10 random numbers. The deficiency of large numbers is evident. It would seem that a not-large-enough Reynolds number could account for the observed results. There are simply not enough steps in the ‘cascade’.

The most serious difficulties with the theory arise when trying to predict rare events or any of the higher moments from the lognormal model. If y is a log-normally distributed variable then the probability density function is given by

$$P(y) = \frac{1}{(2\pi)^{\frac{1}{2}} \sigma y} \exp \left[-\frac{(\ln y - m)^2}{2\sigma^2} \right],$$

where

$$m = \overline{\ln y}$$

and

$$\sigma^2 = \overline{(\ln y)^2} - (\overline{\ln y})^2.$$

The p th moment of this distribution is

$$\overline{\Phi^p} = \int_0^\infty y^p P(y) dy = \exp (pm + \frac{1}{2}p^2\sigma^2).$$

Given m and σ one can therefore predict all moments of the variable y . The coefficient of excess of y will be given by

$$\frac{\mu_4}{\mu_2^2} - 3,$$

where

$$\mu_2 = \overline{\Phi^2} - \bar{\Phi}^2$$

and

$$\mu_4 = \overline{\Phi^4} - 4\overline{\Phi^3}\bar{\Phi} + 6\overline{\Phi^2}\bar{\Phi}^2 - 3\bar{\Phi}^4.$$

Table 2 shows a comparison of the first four moments and the coefficient of excess predicted by the above relations with those calculated directly from the signal. The data is that used in preparing figure 2. Note the enormous values of coefficient of excess predicted by fitting a normal distribution to the logarithm of the observed numbers. The observed values of the coefficient of excess are much smaller (although still very large compared with those from most stochastic data).

Moment	Predicted from log-normal model	Calculated in normal manner
1	0.36	0.29
2	0.41	0.20
3	1.46	0.25
4	16.6	0.47
Coefficient of excess	186	10.6

TABLE 2. Velocity derivative

Kolmogorov similarity theory calls for the skewness of the velocity derivative, shown in table 1, to be an absolute constant—but there is no theory (so far as the authors are aware) predicting its value and no other high Reynolds number data with which to compare it.

There is a direct relation connecting the skewness of the velocity difference at two points separated by a distance r with the Kolmogorov constant K' of the ‘ $-\frac{5}{3}$ ’ region of a one-dimensional downstream velocity spectrum. The relation is

$$S(r) = 0.100(K')^{-\frac{1}{2}}.$$

The condition that this relation holds is that the separation r is small enough that the turbulence is locally isotropic and large enough that viscosity is unimportant. If these lower and upper limits are taken as the peak of the dissipation spectrum and one-tenth the distance of the probe above the water respectively, it can be seen from figure 5 that the value of $S(r)$ is close to 0.26. This can be compared with values of 0.31 calculated from K' by Pond *et al.* (1966) and 0.39 and 0.36 reported by Stewart (1963) as a correction to some values measured by Gurvich (1960). The value of 0.26 corresponds to a Kolmogorov constant K'

of 0.53, which is somewhat higher than what is presently thought to be the proper value.

It should be noted that the third-order structure function falls well below even this value for separations greater than about 10 cm—although the $-\frac{5}{3}$ régime of the spectrum extends to scales of several metres. This is further evidence that the $-\frac{5}{3}$ spectrum at large scales is not related to any Kolmogorov inertial subrange.

The quantity $(u_1 - u'_1)^2$ is, for small separations, a property of the small scale turbulence to which the argument of Gurvich & Yaglom (1967) can be applied. For small separations $|u_1 - u'_1|$ should therefore be a lognormally distributed quantity, it should exhibit the property of 'intermittency' and it should have a significant coefficient of excess. Thus the flatness factor of figure 6 could be interpreted as some sort of measure of the development of the intermittency as a function of scale size. The behaviour displayed is much as would have been expected from this interpretation. The flatness factor increases steadily with decreasing separation. In order to reach the values displayed by the derivative (to -0.69 for skewness and 16 for flatness factor) both skewness and flatness factor must increase greatly between separations corresponding to two digitization intervals—about 2 mm—and the zero separation of the differentiation. At the largest separation used here it is still significantly greater than the Gaussian value of 3.

The one or two points representing the smallest separations in figures 5 and 6 are unreliable; for these the differences in velocity were smaller than the noise associated with the electronics leading to inaccurate distributions.

The spectrum of the square of the downstream velocity derivative in figure 4 shows the predicted power law behaviour over the range of frequencies below the peak of the dissipation spectrum. The slope of the line is -0.65 . This can be compared with the values of -0.62 reported by Pond *et al.* (1963) and -0.6 by Gurvich & Zubkovski (1963).

All of these measurements were in atmospheric boundary layers. There is no real theory to predict the *value* of this power, only indications that there should be some power law. It would be useful to have some measurements in a different type of turbulent field—say a high Reynolds number jet—in order to see whether or not there is some form of universal behaviour of this aspect of turbulent fields.

Conclusions

The lognormal model, while generally describing the distribution of the downstream velocity derivatives in the atmospheric boundary layer, is not sufficiently accurate to permit estimation of probabilities for larger values or to permit calculation of any properties from the predicted higher moments. The skewness of the downstream velocity structure function appears to be slightly smaller than indicated by previous data over a scale range in which a locally isotropic behaviour is *a priori* likely. For the larger scales, where the $-\frac{5}{3}$ law is inexplicably observed to persist in the downwind velocity spectrum, the skewness becomes much smaller. The flatness factor behaves at least qualitatively as would be

expected. The square of the downstream velocity derivative exhibits the predicted power law behaviour with a value of the slope in good agreement with that reported by others.

Most of the data presented here was recorded by Mr F. E. Jerome and Mr J. A. Elliott of the Institute of Oceanography of the University of British Columbia in the course of work with other objectives. The authors wish to express their gratitude. One of us (J. R. W.) was on educational leave from the Marine Sciences Branch of the Federal Department of Energy, Mines and Resources during the course of the work reported here. This work was supported in part by the National Research Council of Canada, the Defence Research Board of Canada and the Meteorological Branch of the Department of Transport.

Note

When this paper was originally presented it included a discussion of some temperature fluctuation data which unfortunately were rather severely contaminated by noise. We have since obtained some much 'cleaner' data which are now being analyzed. While we have as yet seen no reason to modify any of the conclusions reached on the basis of the earlier, poorer data, we consider it advisable to hold back publication of these conclusions until they can be better documented using the new data.

REFERENCES

- GURVICH, A. S. 1960 Measurements of the skewness coefficient for the velocity difference distribution in the bottom layer of the atmosphere. *Dokl. Akad. Sci. USSR* **134**, 1073.
- GURVICH, A. S. & YAGLOM, A. M. 1967 Breakdown of eddies and probability distributions for small-scale turbulence. *Phys. Fluids Suppl.* **10** (part II), S 59.
- GURVICH, A. S. & ZUBKOVSKI, S. L. 1963 *Izv. Akad. Nauk. S.S.S.R. Ser. Geofis.* 1856.
- KOLMOGOROV, A. N. 1941 The local structure of turbulence in an incompressible viscous fluid for very large Reynolds number. *C.R. (Dokl.) Acad. Sci. USSR* **30**, 301.
- KOLMOGOROV, A. N. 1962 A refinement of previous hypothesis concerning the local structure of turbulence in a viscous incompressible fluid at high Reynolds number. *J. Fluid Mech.* **13**, 82.
- NOVIKOV, E. A. & STEWART, R. W. 1964 The intermittency of turbulence and the spectrum of energy dissipation fluctuations. *Izv. Akad. Nauk. Ser. Geophys.* no. 3, 408.
- OBOUKOV, A. M. 1941a *C.R. (Dokl.) Acad. Sci. USSR* **32**, 19.
- OBOUKOV, A. M. 1941b *Izv. Nauk. S.S.S.R., Ser. Geogr. i. Geofiz.* **5**, 453.
- OBOUKOV, A. M. 1962 Some specific features of atmospheric turbulence. *J. Fluid. Mech.* **13**, 77.
- POND, S. 1965 Turbulent spectra in the atmospheric boundary layer over the sea. Unpublished Ph.D. thesis, Institute of Oceanography and Department of Physics, University of British Columbia (IOUBC Manuscript Report no. 19).
- POND, S., SMITH, S. D., HAMBLIN, P. F. & BURLING, R. W. 1966 Spectra of velocity and temperature fluctuations in the atmospheric boundary layer over the sea. *J. Atmos. Sci.* **23**, 376.
- POND, S., STEWART, R. W. & BURLING, R. W. 1963 Turbulent spectra in the wind over waves. *J. Atmos. Sci.* **20**, 319.
- STEWART, R. W. 1963 On the reconciliation of experimental data on the spectrum of locally isotropic turbulence. *Dokl. Akad. Sci. USSR* **152**, 324.